Orthopaedics & Traumatology: Surgery & Research (2013) 99, 80—87

Available online at
SciVerse ScienceDirect
www.sciencedirect.com
Elsevier Masson France
EM|consulte
www.em-consulte.com/en

ORIGINAL ARTICLE

Flatfoot in children and adolescents. Analysis of imaging findings and therapeutic implications

C. Bourdet [a], R. Seringe [b], C. Adamsbaum [c], C. Glorion [d], P. Wicart [d,*]

[a] *Department of pediatric radiology, Paris Descartes University, Cochin — Saint-Vincent-de-Paul Hospital, AP—HP, 27, rue du Faubourg-Saint-Jacques, Paris, France*
[b] *Paris Descartes University, Cochin Hospital, AP—HP, 27, rue du Faubourg-Saint-Jacques, 75014 Paris, France*
[c] *Department of pediatric Radiology, Paris-XI University, Bicêtre Hospital, AP—HP, 78, rue du Général-Leclerc, 94275 Le Kremlin-Bicêtre, France*
[d] *Department of pediatric Orthopaedics, université Paris-Descartes, Necker—Enfants-Malades Hospital, AP—HP, 149—161, rue de Sèvres, 75015 Paris, France*

Accepted: 5 October 2012

KEYWORDS
Flatfoot;
Radiographs;
Children;
Adolescents;
Foot deformities

Summary
Introduction: Pes planovalgus (PPV) is a complex three-dimensional deformity of which routine radiographs provide only a two-dimensional analysis.
Hypothesis: Angles and other radiographic parameters of the foot in children and adolescents, when studied on both the dorsoplantar and the lateral view, can be used to establish a radiographic classification system for PPV that provides useful therapeutic guidance in clinical practice.
Materials and methods: A retrospective single-centre study was conducted on 65 feet in 35 patients aged 7 to 18 years and having adequate ossification. All patients had a clinical diagnosis of idiopathic or neurologic PPV and available weight-bearing dorsoplantar and strict lateral radiographs. We excluded pes planus due to tarsal coalition, congenital bone deformities, or overcorrection of talipes equinovarus ($n = 25$). All possible axes were drawn and angles measured after an evaluation of interindividual agreement.
Results: We identified four patterns of PPV: subtalar pes planus ($n = 16$) with marked subtalar valgus and longitudinal sag predominating at the talonavicular joint, midtarsal pes planus ($n = 12$) without subtalar valgus but with marked midtarsal abduction and sag predominating at the cuneonavicular joint, mixed pes planus ($n = 28$) with subtalar valgus, midtarsal abduction, and sag at both the talonavicular and cuneonavicular joints, and pes planocavus ($n = 9$) with sag of the medial arch and cavus deformity of the lateral arch.
Conclusion: This original classification system provides therapeutic guidance by helping to match the surgical procedure to the nature and location of the deformities.
Level of evidence: Level IV.

* Corresponding author.
E-mail address: p.wicart@nck.aphp.fr (P. Wicart).

1877-0568/$ - see front matter © 2012 Elsevier Masson SAS. All rights reserved.
http://dx.doi.org/10.1016/j.otsr.2012.10.008

Introduction

Pes planovalgus (PPV) is a common deformity that is usually idiopathic but can be caused by neurological, dystrophic, traumatic, or other conditions. Although the term PPV is widely used, to the best of our knowledge, no detailed analysis of the imaging findings is available for investigating any specific characteristics. The only radiological classification system, developed by Tachdjian, relies solely on the lateral radiograph [1]. In a recent analysis of the radiological characteristics of symptomatic and asymptomatic flatfoot, Moraleda and Mubarak found that lateral navicular displacement (assessed based on talonavicular coverage) was the most striking feature of symptomatic flatfoot requiring corrective surgery [2]. However, no attempt was made in their study to identify different radiological patterns of PPV. Knowledge of radiological patterns would provide useful guidance for determining when surgery is appropriate and which procedure is optimal, two points for which there is currently no consensus. Although surgery is rarely performed, many different surgical procedures are used, suggesting the existence of multiple patterns of PPV. Procedures used to correct subtalar joint pronation (calcaneal eversion) and excessive talocalcaneal divergence include permanent [3,4] and temporary [5] subtalar joint arthrodesis using a variety of devices [6,7], arthrodesis at other sites (talonavicular arthrodesis, multiple arthrodeses) [4,8—10], and a variety of extra-articular osteotomies (Evans' osteotomy [11], Mosca's osteotomy [12,13], and Dwyer's calcaneal realignment osteotomy [14]). These methods are often combined with soft-tissue procedures such as shortening of the plantar fascia, lengthening of the Achilles tendon, mid-plantar talonavicular capsulorrhaphy, and correction of abnormal tibialis anterior tendon attachments [4].

The objective of this study was to use radiological parameters to establish a PPV classification system of relevance to the treatment of children and adolescents.

Patients and methods

Inclusion criteria were age between 7 and 18 years, clinical PPV, and availability of weight-bearing lateral and dorsoplantar radiographs. Méary's view (weight-bearing anteroposterior view of the ankle and foot with a metal wire circling the heel) was not obtained routinely. We did not include patients with PPV due to synostosis, congenital bone deformities, or overcorrection of congenital talipes equinovarus.

We included 65 feet in 35 patients with a mean age of 11 ± 2 years (range, 7—18). The diagnosis was idiopathic PPV for 35 feet and secondary PPV, usually due to neurological conditions, for 30 feet. Surgery was performed for 31 feet using a variety of procedures depending on the type of deformity and cause (Table 1).

The radiographs were reviewed independently by a radiologist (CB) and a paediatric orthopaedic surgeon (PW). Several angles were measured on each view. Reference angle values were those reported by Wanderwilde and Staheli [15], the foot radiology atlas [16], Davids [17], and Keats and Sistrom [18].

Table 1 Aetiologies of pes planovalgus (PPV) in our study of 65 feet in 35 patients.

Criteria	$n = 65$
Idiopathic PPV	35
Secondary PPV	30
Charcot-Marie-Tooth	4
West syndrome	2
Ischemic hemiplegia	3
Marfan syndrome	4
Miscellaneous encephalopathies	9
Autism	4
Spastic diplegia (Little's disease)	3
Spastic tetraplegia	1

The following axes were drawn on the weight-bearing dorsoplantar view: axis of the talus (line midway between the medial and lateral edges), axis of the calcaneus (line tangent to the lateral edge) and longitudinal axes of the first and fifth metatarsals (M1 and M5, respectively; lines midway between the medial and lateral edges). Then, the following angles were measured on this view: talocalcaneal divergence ($20^\circ <$ normal $< 25^\circ$), angle subtended by the lateral calcaneal edge and longitudinal axis of M5 (normal, 0°), and angle subtended by the axis of the talus and longitudinal axis of M1 ($0^\circ <$ normal $< 5^\circ$). The talonavicular coverage angle, expressed as a percentage, was formed by the lines perpendicular to the lines through the medial and lateral edges of the talar and navicular joint surfaces [17].

On the lateral view, the following axes were drawn: longitudinal axis of the talus (line bisecting the upper and lower edges), axis of the calcaneus (line tangent to the lower edge of the calcaneus), and longitudinal axes of M1 and M5 (lines parallel to the upper edges). The following angles were measured: calcaneal pitch (between the calcaneus and the ground, $15^\circ <$ normal $< 20^\circ$), talus-M1 angle or Méary's angle ($0^\circ <$ normal $< 10^\circ$), talocalcaneal divergence ($35^\circ <$ normal $< 40^\circ$), calcaneus-M5 angle (normal, 150°—175°), and M1 pitch angle ($10^\circ <$ normal $< 20^\circ$). We did not use the M1-M5 angle, whose discriminating performance is limited.

The apex of the medial sag was identified based on the relative orientations of the talonavicular, cuneonavicular, and cuneiform-M1 joint spaces, as assessed using the following three angles: angle between the longitudinal talar axis and navicular joint surface (normal, 90°), angle between the joint surfaces of the navicular and medial cuneiform (normal, 0°), and angle between the joint surface of the medial cuneiform and M1 (normal, 0°) (Figs. 1 and 2).

Variabilities

Interobserver variability of angle measurement was assessed by having one radiologist (CB) and one paediatric orthopaedic surgeon (PW) evaluate the radiographs of the same 10 feet; subsequently, the angles were measured by these two observers working together. Interindividual concordance rates ranged across angles from 0.85 to 0.95.

Figure 1 Axes drawn and angles measured on the lateral weight-bearing radiograph: analysis of the medial column, lateral column, and talocalcaneal divergence (blue line).

Figure 2 Axes drawn and angles measured on the dorsoplantar weight-bearing radiograph: analysis of talocalcaneal divergence and of the lateral column (red lines).

Statistical analysis

Mean angle values were compared to normal values using the non-parametric Wilcoxon Mann-Whitney test. Values of *P* lower than 0.05 were considered significant.

Results

The clinical results were assessed retrospectively based on notes and photographs taken during clinic visits. All feet were classified clinically by a paediatric orthopaedic surgeon as exhibiting PPV deformity.

Overall, the only parameter that was modified consistently and always in the same direction was Méary's angle (talus-M1), which was consistently increased (mean, $35 \pm 11^{\circ}$).

Talocalcaneal divergence was variable on both the dorsoplantar view (mean, $27 \pm 10^{\circ}$; normal, $15-25^{\circ}$) and the lateral view (mean, $48^{\circ} \pm 10^{\circ}$; normal, $20-30^{\circ}$). Talocalcaneal divergence did not correlate with clinical valgus, which was a consistent feature. Thus, in some cases, this parameter was within the normal range despite the presence of clinical valgus.

Talonavicular coverage (mean, $50 \pm 20\%$) and the talus-M1 angle on the dorsoplantar view ($22 \pm 10^{\circ}$), similar to Méary's angle, had no discriminating potential.

The calcaneus-M5 angle on the dorsoplantar view correlated with rectilinearity of the lateral edge of the foot and with abduction of the forefoot.

An analysis of all the radiological parameters allowed us to identify four patterns of PPV: subtalar, midtarsal, mixed, and planocavus:

- the subtalar pes planus pattern ($n = 16$) was characterised by subtalar valgus with a rectilinear lateral edge of the foot on the dorsoplantar view. On the lateral view, the apex of the flatfoot was the talonavicular joint (Table 2 and Fig. 3);
- the midtarsal pes planus pattern ($n = 12$) was characterised on the dorsoplantar view by marked midtarsal abduction without radiological evidence of subtalar valgus. The apex of the flatfoot on the lateral view was at the cuneiform-navicular joint (Table 3 and Fig. 4);
- the mixed pes planus pattern ($n = 28$) combined subtalar valgus and midtalar abduction on the dorsoplantar view. The apex of the flatfoot on the lateral view was shared by the talonavicular and cuneonavicular joints (Table 4 and Fig. 5);
- the pes planus cavus pattern ($n = 9$) combined a cavus deformity of the lateral arch on the lateral view (increased calcaneus-M5 angle) and sag of the medial arch. The dorsoplantar view showed moderate midtarsal abduction (Table 5 and Fig. 6).

In non-idiopathic static flatfoot, the radiological presentation was more complex, with participation of both the subtalar and the midtalar joints in the deformity. Neurological conditions were responsible for 20 of the 28 mixed pes planus deformities (Table 6).

Inadequate talonavicular coverage, as assessed by the talonavicular angle on the dorsoplantar view, correlated with mid- and forefoot abduction and with subtalar valgus.

Discussion

Our radiographic analysis shows that the term ''pes planovalgus'' encompasses several different deformities. We developed a simple classification system with four patterns that have different surgical requirements. This classification should also prove useful for adults with flatfoot, since radiological parameters are the same in adolescents and in adults.

A drawback of our classification system is failure to take into account a possible contribution of the talocrural joint to the valgus deformity, which could be detected on the Méary anteroposterior view of the hindfoot (weight-bearing anteroposterior view of the ankle and foot with a metal wire circling the heel). The presence in some feet of clinical

Table 2 Subtalar pes planovalgus ($n = 16$): subtalar valgus, little or no mid-tarsal abduction and talonavicular location of the medial-arch sag.

Parameters	Angles	Mean ± SD	Normal values	Interpretation	*P* value
DP	A. Talus-calcaneus	34 ± 4°	20–30°	↗	0.0003
DP	A. Calcaneus-M5	0 ± 2°	0°	N	0.08
Face	Talonavicular coverage (index, as a %)	48 ± 15%	0°	↗	0.02
Lateral	A. Talus-navicular surface	70 ± 8°	90°	↘	0.001
Lateral	A. Navicular surface - 1st cuneiform surface	5 ± 5°	0°	N	0.5
Lateral	A. Calcaneus-M5	165 ± 7°	160°	N	0.006

DP: dorsoplantar view; M5: fifth metatarsal; A.: angle.

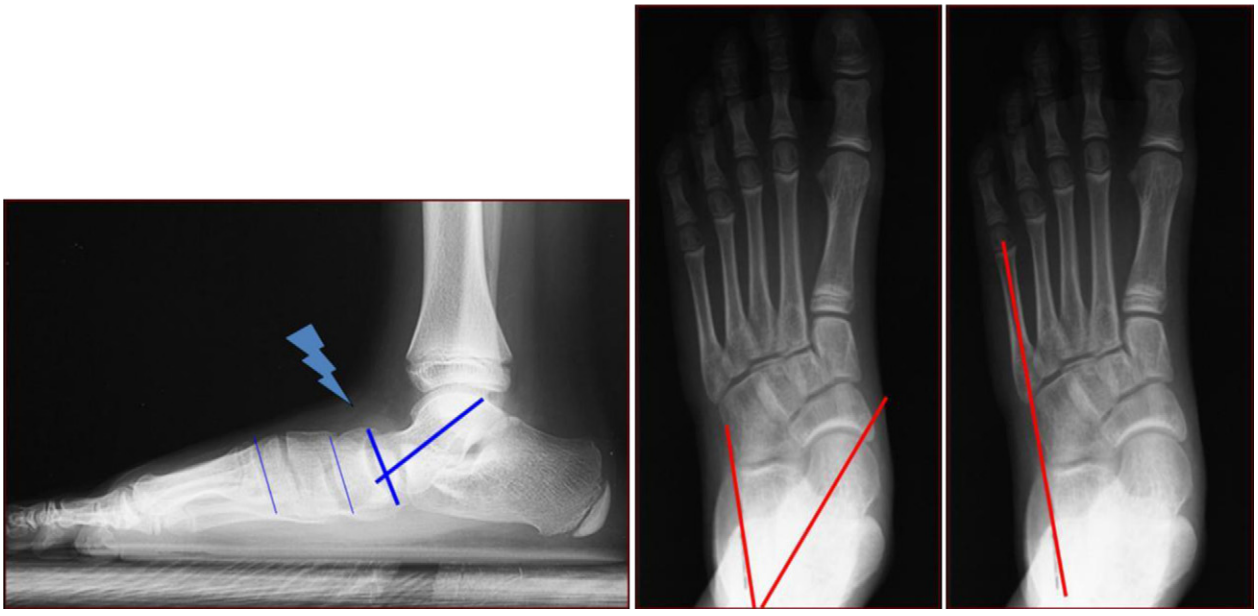

Figure 3 Subtalar pes planovalgus, dorsoplantar and lateral views showing the subtalar valgus with little or no midtarsal abduction and talonavicular location of the medial-arch sag.

Table 3 Midtarsal pes planovalgus ($n = 12$): no subtalar valgus, marked midtarsal abduction, and cuneonavicular location of the medial-arch sag.

Parameters	Angles	Mean ± SD	Normal values	Interpretation	*P* value
DP	A. Talus-calcaneus	19 ± 2°	25°	N	0.009
DP	A. Calcaneus-M5	16 ± 5°	0°	↗	1
DP	Talonavicular coverage (index, as a %)	57 ± 15%	0°	↗	0.03
Lateral	A. Talus-navicular surface	87 ± 4°	90°	N	0.03
Lateral	A. Navicular surface – 1st cuneiform surface	15 ± 4°	0°	↗	0.03
Lateral	A. Calcaneus-M5	162 ± 8°	160°	N	1

DP: dorsoplantar view; M5: fifth metatarsal; A.: angle.

hindfoot valgus with no increase in radiological talocalcaneal divergence is probably ascribable to valgus at the talocrural joint.

Furthermore, faultless technique should be used when obtaining the radiographs. Only full weight-bearing views should be used. For instance, radiographs obtained with one foot placed anteriorly to the other (Egyptian stance) are not interpretable.

Méary's angle (talus-M1 on the lateral view) did not contribute to discriminate among the patterns in our classification system. This parameter reflected only the severity of the overall medial-arch sag. It was not specific

Figure 4 Midtarsal pes planovalgus, dorsoplantar and lateral views showing the absence of subtalar valgus and the marked midtarsal abduction and cuneonavicular location of the medial-arch sag.

Table 4 Mixed pes planovalgus ($n = 28$): subtalar valgus, midtarsal abduction, and dual talonavicular and cuneonavicular location of the medial arch sag.

Parameters	Angles	Mean ± SD	Normal values	Interpretation	*P* value
DP	A. Talus-calcaneus	32 ± 4°	25°	↗	0.04
DP	A. Calcaneus-M5	14 ± 7°	0°	↗	0.03
DP	Talonavicular coverage (index, as a %)	50 ± 15%	0°	↗	0.01
Lateral	A. Talus-navicular surface	80 ± 5°	90°	↘	0.016
Lateral	A. Navicular surface - 1st cuneiform surface	10 ± 5°	0°	↗	0.016
Lateral	A. Calcaneus-M5	160 ± 20°	160°	N	0.19

DP: dorsoplantar view; M5: fifth metatarsal; A.: angle.

Table 5 Pes planocavus ($n = 9$): shortened lateral arch, moderate midtarsal abduction, normal calcaneal pitch, and talonavicular and/or cuneonavicular location of the medial-arch sag.

Parameters	Angles	Mean ± SD	Normal values	Interpretation	*P* value
DP	A. Talus-calcaneus	24 ± 7°	25°	N	0.9
DP	A. Calcaneus-M5	16 ± 9°	0°	↗	0.04
DP	Talonavicular coverage (index, as a %)	35 ± 20%	0°	↗	0.04
Lateral	A. Talus-navicular surface	83 ± 10°	90°	N or ↘	0.5
Lateral	A. Navicular surface — 1st cuneiform surface	10 ± 8°	0°	N or ↗	0.04
Lateral	A. Calcaneus-M5	145 ± 5°	160°	↘	0.04
Lateral	A. Calcaneal pitch	24 ± 19°	20°	N	0.55

DP: dorsoplantar view; A.: angle.

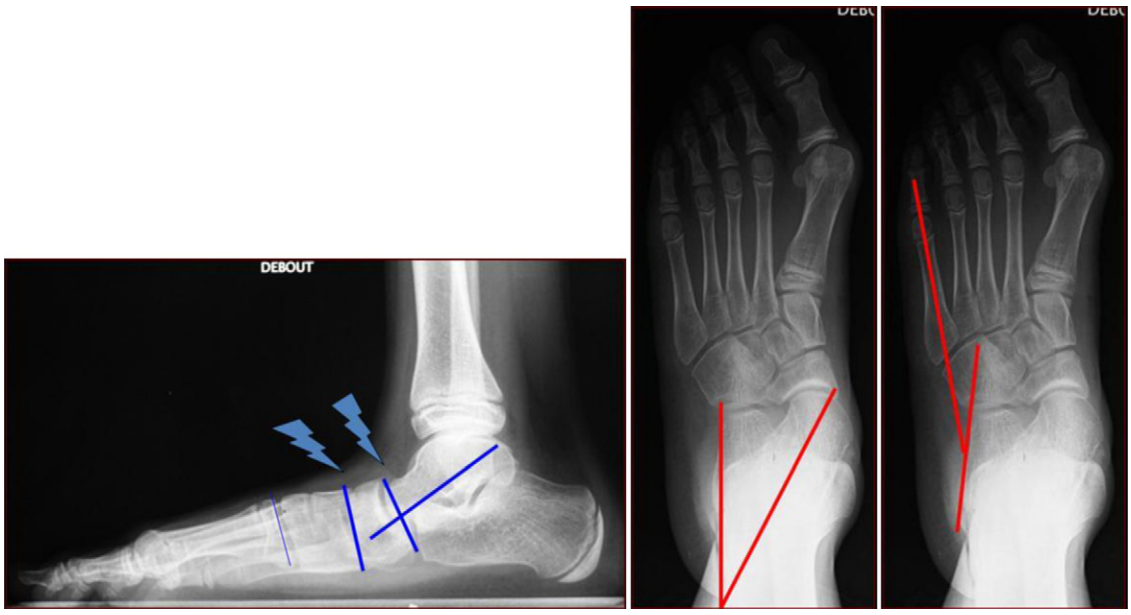

Figure 5 Mixed pes planovalgus, dorsoplantar and lateral views showing the subtalar valgus, midtarsal abduction, and dual talonavicular and cuneonavicular location of the medial-arch sag.

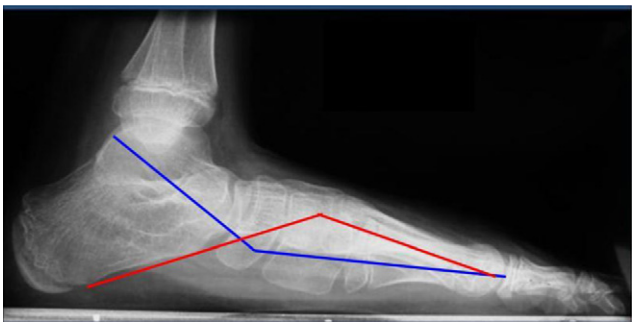

Figure 6 Pes planocavus, lateral view showing the sag medial column and high-arched lateral column.

of any particular joint deformity but instead reflected the presence of deformities affecting the talonavicular, cuneiform-navicular, cuneiform-metatarsal, and subtalar joints.

The inadequate talonavicular coverage seen in both the subtalar and the midtarsal patterns illustrates the fact that the talonavicular joint belongs both to the subtalar articular complex and to the mid-tarsal joint [19,20]. This fact, which is crucial to a good analysis of foot deformities, explains that neither inadequate talonavicular coverage nor talus-M1 angle abnormalities on the dorsoplantar view contributed to improve the specificity of the diagnosis. In contrast, many earlier studies concluded that talonavicular coverage reflected only midfoot and/or forefoot deformities [2,15,17,18].

In our classification system, a careful analysis of the parallelism of the medial-column joint lines described by Tachdjian [1], in contrast, is crucial to correlate the antero-posterior deformities with the pattern of medial-arch sag on the lateral view, a point that was not described by Tachdjian.

Table 6 Correlation between the pes planovalgus pattern in our classification system and the aetiology of the deformity.

Type	Idiopathic ($n = 35$) (%)	Secondary ($n = 30$) (%)
Subtalar PPV ($n = 16$)	12 (34)	4 (16)
Midtarsal PPV ($n = 12$)	10 (29)	2 (2)
Mixed PPV ($n = 28$)	8 (23)	20 (66)
Pes planocavus ($n = 9$)	5 (14)	4 (16)

PPV: pes planovalgus.

Subtalar PPV

A good understanding of midtarsal PPV requires a consideration of the calcaneopedal unit (CPU) and talar-tibial-fibular unit (TTFU) [19]. The TTFU rotates medially above the CPU, which is initially free of any intrinsic deformities, as suggested by the normal calcaneal-M5 angle on the dorsoplantar view. This rotational displacement occurs within the subtalar articular complex composed of the subtalar and talonavicular joints, a fact that explains the increased talocalcaneal divergence and talonavicular subluxation, respectively. As expected, the apex of the flatfoot is at the talonavicular joint, which is the most clearly visible component of the subtalar articular complex on the lateral view.

Midtarsal PPV

Midtarsal PPV is characterised by abnormal CPU shape with the apex of the flatfoot at the cuneiform-navicular joint and abduction of the midtarsal joint. The resulting transverse tarsal abnormality also decreases the talonavicular coverage, illustrating the contribution of this joint to both the subtalar articular complex and the transverse tarsal joint.

In contrast, the talocalcaneal joints contribute little to this pattern of PPV.

Mixed PPV

Mixed PPV combines the changes seen in subtalar and midtarsal PPV.

Pes planocavus

Pes cavus is a distinct entity in which the medial column is collapsed and the lateral column has an abnormally high arch. The loss of talonavicular coverage is less marked than in the other PPV patterns, talocalcaneal divergence is limited, and calcaneal pitch is normal or increased. In this case, the location of the flatfoot apex was variable (talonavicular joint in 3 feet, cuneiform-navicular joint in 4 feet, and mixed in 2 feet). However, moderate midtarsal abduction was a consistent finding in the pes planocavus pattern.

Therapeutic implications

Our new classification system for PPV is useful for guiding surgical decisions. Subtalar PPV is a good indication for subtalar procedures such as the Grice procedure (no longer used given the arthrodesis) [21], temporary subtalar joint arthrodesis [5], or subtalar implant [6]. In contrast, calcaneal lengthening osteotomy [11,13] does not make sense in this PPV pattern, as it would result in convexity of the lateral edge of the foot (by adduction of the forefoot) manifesting as inversion of the calcaneal-M5 angle on the dorsoplantar view. Calcaneal lengthening osteotomy [11,13] is the procedure of choice for midtarsal PPV, to correct the concavity of the lateral edge of the foot (forefoot abduction) and to restore adequate talonavicular coverage while also decreasing the talocalcaneal divergence [22]. Complementary medial column osteotomy is often in order to better correct both the medial-arch sag and the hindfoot supination [13,23]. Osteotomy of the cuneiform bones may be inadvisable, as the result is a sagittal bayonet deformity that can produce a dorsal bulge responsible for difficulties with footwear, and also because the sag is located at the talonavicular joint. Talonavicular surgery would result in the equivalent of triple arthrodesis, due to the contribution of this joint to both the subtalar articular complex and the mid-tarsal joint, and therefore should not be performed. Intra-navicular surgery allows only a small degree of angle correction that is usually not satisfactory. In contrast, plantar and medial closing osteotomy of the cuneonavicular joint has a number of benefits. This joint is near the architectural abnormality, and the proximal site of the osteotomy allows a considerable degree of angle correction. However, arthrodesis is required and eliminates a non-negligible amount of mobility [24].

Pes planus cavus is an absolute contraindication to calcaneal lengthening, which would exacerbate the cavus deformity of the lateral column. In contrast, shortening osteotomy of the medial column (plantar and medial closing osteotomy of the cuneonavicular joint) is logical, to correct the abduction and arch sag.

In conclusion, this original study provides a detailed analysis of the radiological abnormalities seen in PPV and provides a rationale for choosing the best treatment. The use of 3D weight-bearing imaging systems (e.g., EOS®) [25] will probably allow further refinements to our analysis and constitutes a promising avenue of research.

Disclosure of interest

The authors declare that they have no conflicts of interest concerning this article.

References

[1] Tachdjian M. The child's foot. Saunders Co; 1985. p. 556—97.
[2] Moraleda L, Mubarak SJ. Flexible flatfoot: Differences in the relative alignment of each segment of the foot between symptomatic and asymptomatic patients. J Pediatr Orthop 2011;31:421—8.
[3] Grice DS. An extra-articular arthrodesis of the subastragalar joint for correction of paralytic flat feet in children. J Bone Joint Surg Am 1952;34:927—40.
[4] Biga N, Mouliès D, et Mabit C. Pied plat valgus statique (y compris les synostoses congénitales). EMC Appareil locomoteur 1999:10 [14-110-A-10, In French].
[5] Judet J, Largier A, Pouliquen JC. L'opération de cavalier dans le traitement des pieds plats valgus graves. In: Judet R, editor. Actualités de chirurgie orthopédique XIII. Paris: Masson; 1976. p. 109—19 [In French].
[6] Giannini S, Girolami M, Ceccarelli F. The surgical treatment of infantile flat foot: a new expanding endo-orthotic implant. Ital J Orthop Traumatol 1985;11:315—22.
[7] Husain ZS, Fallat LM. Biomechanical analysis of Maxwell—Brancheau arthroereisis implants. J Foot Ankle Surg 2002;41:352—8.
[8] Hoke M. An operation for the correction of extremely relaxed flat feet. J Bone Joint Surg 1931;13:773—83.
[9] Adelaar RS, Dannelly EA, Meunier PA, Stelling FH, Goldner JL, Colvard DF. A long term study of triple arthrodesis in children. Orthop Clin North Am 1976;7:895—908.
[10] Saltzman CL, Fehrle MJ, Cooper RR, Spencer EC, Ponseti IV. Triple arthrodesis: twenty-five and forty-four-year average follow-up of the same patients. J Bone Joint Surg Am 1999;81:1391—402.
[11] Evans D. Calcaneo-valgus deformity. J Bone Joint Surg Br 1975;57:270—8.
[12] Mosca VS. Calcaneal lengthening for valgus deformity of the hindfoot. Results in children who had severe, symptomatic flatfoot and skewfoot. J Bone Joint Surg Am 1995;77:500—12.
[13] Mosca VS. Calcaneal lengthening osteotomy for valgus deformity of the hindfoot. In: Skaggs DL, Tolo VT, editors. Master techniques in orthopaedic surgery: pediatrics. Philadelphia: Lippincott Williams& Wilkins; 2008. p. 263—76.
[14] Dwyer FC. Osteotomy of the calcaneum for pes cavus. J Bone Joint Surg Br 1959;41:80—6.
[15] Vanderwilde R, Staheli LT. Measurements on radiographs of the foot in normal infants and children. J Bone Joint Surg Am 1988;70:407—14.
[16] Montagne J. Atlas de radiologie du pied. Paris: Masson; 1980 [In French].

[17] Davids JR. Quantitative segmental analysis of weight-bearing radiographs of the foot and ankle for children. J Pediatr Orthop 2005;25:769—76.
[18] Keats TE, Sistrom C. Atlas of radiologic measurements. Philadelphia: Mosby; 2001. p. 293—303.
[19] Seringe R, Wicart P, Judet T. Le bloc calcanéopédieux. In: Les déformations du pied de l'enfant et de l'adulte. Cahiers d'Enseignement de la SOFCOT. Paris: Elsevier Masson SAS; 2010. p. 23—30, [In French].
[20] Sarrafian S. Anatomy of the foot and ankle. Philadelphia: Lippincott Cie; 1983.
[21] Ross PM, Lyne ED. The Grice procedure: indications and evaluation of long-term results. Clin Orthop Rel Res 1980;153:194—200.
[22] Dumontier TA, Falicov A, Mosca V, Sangeorzan B. Calcaneal lengthening: investigation of deformity correction in a cadaver flatfoot model. Foot Ankle Int 2005;26: 166—70.
[23] Rathjen KE, Mubarak SJ. Calcaneal-cuboid-cuneiform osteotomy for the correction of valgus foot deformities in children. J Pediatr Orthop 1998;18:775—82.
[24] Lundgren P, Nester C, Liu A, Arndt A, Jones R, Stacoff A, et al. Invasive in vivo measurement of rear-, mid-, and forefoot motion during walking. Gait posture 2008;28: 93—100.
[25] Kalifa G, Adamsbaum C. Evaluation of a new low-dose digital x-ray device: first dosimetric and clinical results in children. Pediatr Radiol 1998;28:557—61.